Gas-phase association reactions of fullerene cations: modelling the influence of charge state and other molecular parameters on association efficiency

SIMON PETRIE AND DIETHARD K. BOHME[1]

Department of Chemistry and Centre for Research in Earth and Space Science, York University, North York, ON M3J 1P3, Canada

Received July 2, 1993

This paper is dedicated to Professor John C. Polanyi on the occasion of his 65th birthday

SIMON PETRIE and DIETHARD K. BOHME. Can. J. Chem. **72**, 577 (1994).

The efficiency of association reactions of fullerene cations observed in helium at pressures of 0.35–0.4 Torr sustained in a Selected-Ion Flow Tube (SIFT) at room temperature has been examined with a view to the influence of the charge state and the size of the fullerene ion and the size, structure, and degree of unsaturation of the neutral. The association efficiency is found to be strongly dependent on these molecular parameters. The calculated lifetime of the intermediate collision complex provides insight into the well depth associated with the formation of this complex and the effectiveness of vibrational and (or) rotational degrees of freedom of the reactants in the dispersal of the energy of complex formation. The results are considered in terms of single-well and double-well models for the potential energy surface leading to association and are best accommodated by the double-well model involving the formation of an initial electrostatic collision complex that must overcome a barrier to proceed to the formation of a chemically bonded adduct. The observed competition between association and charge transfer can also be accommodated with a double-well model, which provides a lower limit for the depth of the electrostatic well for those systems that exhibit such competition.

SIMON PETRIE et DIETHARD K. BOHME. Can. J. Chem. **72**, 577 (1994).

Dans le but de déterminer l'influence de l'état de la charge, de la grosseur de l'ion fullerène et la grosseur, la structure et le degré d'insaturation de l'espèce neutre, on a étudié l'efficacité des réactions d'association des cations de fullerène observées dans l'hélium, à des pressons de 0,35–0,4 Torr, et qui se produisent dans un tube à écoulement d'ion choisi (SIFT), à la température ambiante. On a trouvé que l'efficacité de l'association varie beaucoup avec ces paramètres moléculaires. Le temps de vie calculé du complexe de collision intermédiaire fournit des données sur la profondeur du puits associé à la formation de ce complexe et sur l'efficacité des degrés de liberté vibrationnels et (ou) rotationnels des réactifs dans la dispersion de l'énergie de formation du complexe. On considère les résultats en fonction des modèles à un et à deux puits pour la surface d'énergie potentielle conduisant à l'association et ils s'accommodent mieux avec le modèle à double puits impliquant la formation d'un complexe de collision électrostatique initial qui doit vaincre une barrière avant de procéder à la formation d'un adduit chimiquement lié. La compétition observée entre l'association et le transfert de charge peut aussi être accommodée avec un modèle à double puits qui fournit une limite inférieure pour la profondeur du puits électrostatique des systèmes qui présentent une telle compétition.

[Traduit par la rédaction]

Introduction

The occurrence of bond formation is a central feature of chemistry. The process of association

[1] $$\mathrm{A + B \longrightarrow AB}$$

is the most direct means of chemical bond formation, and a study of the kinetics of association therefore offers insight into the factors affecting the efficiency of bond formation.

The laboratory study of the kinetics of association reactions in the gas phase has been dominated by the investigation of ion–molecule association processes

[2] $$\mathrm{A^+ + B \longrightarrow AB^+}$$

for two reasons. Firstly, ion–molecule reactions are easily studied by a variety of mass-spectrometric techniques (1). Secondly, owing to the attractive ion–dipole and ion – induced dipole interaction (2), ion–molecule reactions are generally of higher efficiency than neutral–neutral reactions (which are often inhibited by activation energy barriers).

Reactions of type [2] are also possible with multiply charged species A^{n+}, and indeed some examples of association reactions of simple (atomic and diatomic) gas-phase dications have been reported (3–5). However, ions bearing multiple charges are often prone to Coulomb explosion and, because of their relatively high appearance energies, their association with molecules must often compete with other processes: charge transfer or dissociative charge transfer in the case of multiply charged atomic and diatomic ions and proton transfer in the case of hydrogenated polyatomic ions. For these reasons, it has not been possible to examine the kinetics of association for multiply charged ions in any detail. Indeed, there appear to have been no previous measurements of reactions of type [2] involving trications A^{3+} or ions of higher charge state.

This situation has changed with the availability of Buckminsterfullerene, C_{60} (6). It is now relatively easy to produce the stable cations $C_{60}^{\cdot+}$, C_{60}^{2+}, $C_{60}^{\cdot 3+}$, C_{60}^{4+}, and $C_{60}^{\cdot 5+}$ in the laboratory for experimental study (7–9), so that a unique opportunity has arisen to explore the physicochemical aspects of association as a function of the reactant ion charge state. To this end, we previously reported the first quantitative measurements of the kinetics of association reactions involving the ions $C_{60}^{\cdot+}$, C_{60}^{2+}, and $C_{60}^{\cdot 3+}$ (10–18). For example, we characterized primary and higher order association leading to the formation of single-, double-, and triple-handled adducts as typified by structures **I** (10), **II** (13), and **III** (15).

Here we shall focus on selected-ion flow tube (SIFT) measurements on ion–molecule reactivity previously performed in our laboratory upon the fullerene ions $C_{60}^{\cdot+}$, C_{60}^{2+}, $C_{60}^{\cdot 3+}$, C_{56}^{n+}, C_{58}^{n+}, and C_{70}^{n+} (n = 1, 2) (10–18). We shall use the

---

[1] Author to whom correspondence may be addressed.

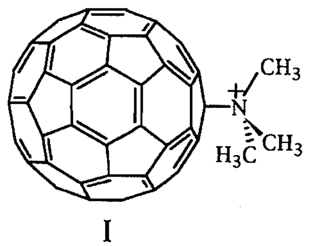

I

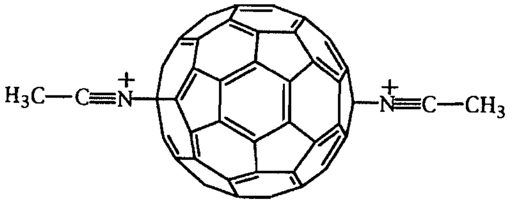

II

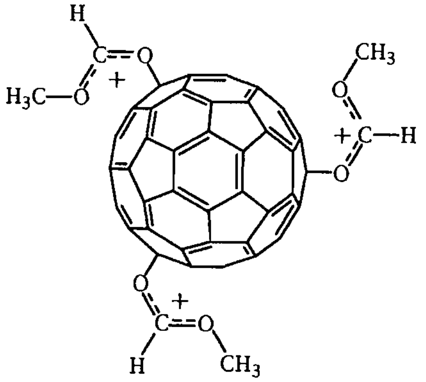

III

results of these studies to investigate the dependence of association efficiency upon the physical parameters of the reactants (ion size and charge state; neutral size, structure, and degree of unsaturation), and hence to infer the nature of the potential energy surface leading to association. Furthermore, a number of systems are considered in which competing bimolecular channels have been observed. Our primary objective is to obtain an overall perspective for a range of novel association reactions involving fullerene ions and various neutral molecules.

Discussion

We previously reported a large number of reactions of the fullerene cations C_{60}^{n+} (n = 1, 2, 3) (10–18). Some of these results are presented in Tables 1–5. These tables are arranged to illuminate the general features of the efficiency of bond formation with fullerene ions: the influence of charge state, ion size, neutral size, degree of unsaturation of the neutral, and its structure. As is customary, we have defined the efficiency as the ratio of the measured effective bimolecular reaction rate coefficient to the calculated collision rate coefficient, $k(2)_{obs}/k_c$.

The pressure dependence of the efficiency of association has not been investigated systematically. However, results observed for the reaction of $C_{60}^{\bullet +}$ with ethylamine (10) and the reaction of C_{60}^{2+} with allene (11) have indicated that, for these systems, collisional stabilization, eq. [3]:

$$[3] \qquad C_{60}^{n+} + X + M \longrightarrow C_{60}.X^{n+} + M^*$$

dominates over radiative stabilization, eq. [4]:

$$[4] \qquad C_{60}^{n+} + X \longrightarrow C_{60} \cdot X^{n+} + h\nu$$

at the pressures of our SIFT experiments.

A few association reactions with multiply charged fullerene cations have been observed with other experimental techniques but these observations have been entirely qualitative. McElvany et al. (7, 21) used the FT–ICR technique to observe the occurrence of the association reactions

$$[5] \qquad C_{56}^{\bullet 3+} + C_2H_2 \longrightarrow C_{56} \cdot C_2H_2^{\bullet 3+}$$

$$[6] \qquad C_{60}^{\bullet 3+} + C_2H_2 \longrightarrow C_{60} \cdot C_2H_2^{\bullet 3+}$$

Garvey and co-workers (22) inferred the occurrence of the association reaction

$$[7] \qquad C_{60}^{2+} + NH_3 \longrightarrow C_{60} \cdot NH_3^{2+}$$

in a triple quadrupole MS/MS/MS apparatus, although the dicationic adduct $C_{60} \cdot NH_3^{2+}$ was not directly observable in their experiments. We have observed reaction [7] directly (9). Also, our observation of repeated association of 1,3-butadiene (16)

$$[8] \qquad C_{60} \cdot (C_4H_6)_n^{2+} + C_4H_6 \longrightarrow C_{60} \cdot (C_4H_6)_{n+1}^{2+}$$

for n = 0–5 was recently duplicated by Schwarz and co-workers[2] for n = 0–2 in an FT–ICR cell. The observation of the addition reactions [5], [6], and [8] under FT–ICR conditions ($P \sim 10^{-7}$–10^{-3} Torr; 1 Torr = 133.3 Pa) suggests that these reactions may be occurring in a bimolecular fashion by radiative association as in eq. [4].

A. Empirical correlations

Charge state of the fullerene ion

The efficiency of association increases dramatically with increasing charge, as shown in the values reported in Table 1. An increase in association efficiency of ~3 orders of magnitude operates for an increase in charge state from +1 to +2 for the reactions with NH_3 and n-C_3H_7CN, or from +2 to +3 for the reactions with HCN and C_2H_2. This enhancement in reaction efficiency with charge state is larger than (although within experimental uncertainty of) the factor of 100–500 found for the enhancement in association efficiency for reactions of M^{n+} (M = Mg, Ca, Ba; n = 1, 2) with H_2O, N_2, CO, CO_2, N_2O, and O_2 (3). For those reactions of C_{60}^{2+} that exhibit association with near unit efficiency, an enhancement in efficiency with increasing charge state from +2 to +3 is not observable. Similarly, an enhancement in efficiency is not experimentally observable when two successive charge states are both seen to be unreactive as is the case for the reactions of $C_{60}^{\bullet +}$ and C_{60}^{2+} with HCN and C_2H_2.

Size of the fullerene ion

The efficiency of association with various neutrals is noted in Table 2 for the species C_{56}^{n+}, C_{58}^{n+}, C_{60}^{n+}, and C_{70}^{n+}. Association is seen to be much more efficient for C_{56}^{n+} and C_{58}^{n+} than for the slightly larger ion C_{60}^{n+}, which in turn undergoes association with somewhat higher efficiency than C_{70}^{n+}.

---

[2] H. Schwarz, personal communication.

TABLE 1. Effect of ion charge state upon fullerene ion–molecule association reaction efficiency

Reaction[a]	k_c[a]	$k(2)_{obs}$[c]	$k(3)_{obs}$[d]	$k(2)/k_c$[e]	$\tau(\beta = 0.03)$[f]	$\tau(\beta = 1.0)$[f]
$C_{60}^{\cdot +}$ + HCN	2.12	<0.001[g]	<0.009[h]	<0.0005	<0.003	<0.00008
C_{60}^{2+} + HCN	4.23	<0.001[g]	<0.009[h]	<0.0003	<0.0007	<0.00002
$C_{60}^{\cdot 3+}$ + HCN	6.35	2.5[g]	22	0.39	0.76	0.023
$C_{60}^{\cdot +}$ + C_2H_2	0.89	<0.001[i]	<0.008[h]	<0.0011	<0.005	<0.0002
C_{60}^{2+} + C_2H_2	1.78	<0.001[i]	<0.008[j]	<0.0006	<0.0013	<0.00004
$C_{60}^{\cdot 3+}$ + C_2H_2	2.67	0.15[k]	1.3	0.056	0.10	0.0031
$C_{60}^{\cdot +}$ + NH_3	1.69	<0.001[l]	<0.009[j]	<0.0006	<0.004	<0.0001
C_{60}^{2+} + NH_3	3.37	1.2[l]	10	0.36	0.93	0.028
$C_{60}^{\cdot 3+}$ + NH_3	5.04	3.9[l]	>34[m]	0.77	>1	>0.04
$C_{60}^{\cdot +}$ + n-C_3H_7CN	2.08	<0.001[g]	<0.009[h]	<0.0005	<0.003	<0.00008
C_{60}^{2+} + n-C_3H_7CN	4.15	3.9[g]	>34[m]	0.94	>2	>0.07
$C_{60}^{\cdot 3+}$ + n-C_3H_7CN	6.23	6.3[g]	>55[m]	1.0	>1	>0.05

[a] Addition reaction, studied using the SIFT technique at a temperature of 294 ± 2 K and at a helium buffer gas pressure of 0.35 ± 0.01 Torr unless otherwise specificed.

[b] ADO collision rate coefficient in units of 10^{-9} cm^3 molecule^{-1} s^{-1}, calculated according to the method of Su and Bowers (19).

[c] Observed effective bimolecular rate coefficient for addition, in units of 10^{-9} cm^3 molecule^{-1} s^{-1}.

[d] Termolecular rate coefficient, in units of 10^{-26} cm^6 molecule^{-2} s^{-1}, calculated from $k(2)_{obs}$. A lower limit to $k(3)_{obs}$ has been assigned to those reactions for which association accounts for ≥50% of collisions, since these reactions are presumed to be saturated at the experimental buffer gas pressure used.

[e] Association efficiency, as defined in the text.

[f] Collision complex lifetime in units of 10^{-6} s, calculated from the termolecular rate coefficient $k(3)_{obs}$ for the factor β as shown for the efficiency of collisional stabilization by helium.

[g] Rate coefficients previously reported in ref. 13.

[h] Upper limit assigned to termolecular rate coefficient, association efficiency, and collision complex lifetime; no association was observed.

[i] Rate coefficients previously reported in ref. 11.

[j] Upper limit assigned to termolecular rate coefficient, association efficiency, and collision complex lifetime; association was observed to occur.

[k] Rate coefficients previously reported in ref. 20.

[l] Rate coefficients previously reported in ref. 10.

[m] Lower limit assigned to termolecular rate coefficient, association efficiency, and collision complex lifetime; association is presumed to be saturated at the operating pressure of these experiments.

TABLE 2. Effect of fullerene ion size upon ion–molecule association reaction efficiency

Reaction[a]	k_c[a]	$k(2)_{obs}$[a]	$k(3)_{obs}$[a]	$k(2)/k_c$[a]	$\tau(\beta = 0.03)$[a]	$\tau(\beta = 1.0)$[a]
C_{56}^{2+} + C_2H_4	1.86	0.021[b]	0.18	0.011	0.031	0.00092
C_{58}^{2+} + C_2H_4	1.86	0.019[b]	0.17	0.010	0.028	0.00084
C_{60}^{2+} + C_2H_4	1.86	<0.001[c]	<0.008[d]	<0.0006	<0.001	<0.00004
$C_{56}^{\cdot +}$ + NH_3	1.69	0.0096[b]	0.084	0.0057	0.031	0.00093
$C_{58}^{\cdot +}$ + NH_3	1.69	0.034[b]	0.30	0.020	0.11	0.0033
$C_{60}^{\cdot +}$ + NH_3	1.69	<0.001[e]	<0.009[d]	<0.0006	<0.004	<0.0001
C_{56}^{2+} + CH_3CN	4.70	4.3[b]	>37[f]	0.91	>2	>0.07
C_{58}^{2+} + CH_3CN	4.69	4.2[b]	>37[f]	0.90	>2	>0.07
C_{60}^{2+} + CH_3CN	4.68	0.080[g]	0.70	0.017	0.047	0.0014
C_{70}^{2+} + CH_3CN	4.66	0.029[g]	0.25	0.0062	0.017	0.00051
C_{60}^{2+} + CH_2CCH_2	1.85	0.080[c]	0.61	0.043	0.10	0.0031
C_{70}^{2+} + CH_2CCH_2	1.85	0.009[c]	0.069	0.005	0.012	0.00034

[a] See footnotes *a–f* for Table 1.

[b] Rate coefficients previously reported in ref. 18.

[c] Rate coefficients previously reported in ref. 11.

[d] Upper limit assigned to termolecular rate coefficient, association efficiency, and collision complex lifetime; asociation was observed to occur.

[e] Rate coefficients previously reported in ref. 10.

[f] Lower limit assigned to termolecular rate coefficient, association efficiency, and collision complex lifetime; association is presumed to be saturated at the operating pressure of these experiments.

[g] Rate coefficients previously reported in ref. 13.

TABLE 3. Effect of neutral reactant size upon fullerene ion–molecule association reaction efficiency

Reaction[a]	k_c[a]	$k(2)_{obs}$[a]	$k(3)_{obs}$[a]	$k(2)/k_c$[a]	$\tau(\beta = 0.03)$[a]	$\tau(\beta = 1.0)$[a]
$C_{60}^{\cdot+} + NH_3$	1.69	<0.001[b]	<0.009[c]	<0.0006	<0.004	<0.0001
$C_{60}^{\cdot+} + CH_3NH_2$	1.44	0.015[b]	0.13	0.010	0.060	0.0018
$C_{60}^{\cdot+} + C_2H_5NH_2$	1.34	0.050[b]	0.43	0.037	0.21	0.0064
$C_{60}^{\cdot+} + (CH_3)_2NH$	1.22	0.85[b]	>7.4[d]	0.70	>4	>0.1
$C_{60}^{\cdot+} + (CH_3)_3N$	1.05	1.0[b]	>8.7[d]	0.95	>5	>0.15
$C_{60}^{2+} + HCN$	4.23	<0.001[e]	<0.009[f]	<0.0003	<0.0007	<0.00002
$C_{60}^{2+} + CH_3CN$	4.68	0.080[e]	0.70	0.017	0.047	0.0014
$C_{60}^{2+} + CH_3CH_2CN$	4.41	2.5[e]	0.57	>22[d]	>1.5	>0.04
$C_{60}^{2+} + n\text{-}C_3H_7CN$	4.15	3.9[e]	>34[d]	0.94	>2	>0.07
$C_{60}^{2+} + i\text{-}C_3H_7CN$	3.93	4.3[e]	>37[d]	1.1	>3	>0.09
$C_{60}^{2+} + C_2H_4$	1.86	<0.001[g]	<0.008[c]	<0.0006	<0.001	<0.00004
$C_{60}^{2+} + C_3H_6$	1.98	1.3[g]	>10[d]	0.66	>1	>0.04
$C_{60}^{2+} + 1\text{-}C_4H_8$	1.94	2.2[g]	>17[d]	1.1	>2	>0.08

[a] See footnotes *a–f* for Table 1.

[b] Rate coefficients previously reported in ref. 10.

[c] Upper limit assigned to termolecular rate coefficient, association efficiency, and collision complex lifetime; association was observed to occur.

[d] Lower limit assigned to termolecular rate coefficient, association efficiency, and collision complex lifetime; association is presumed to be saturated at the operating pressure of these experiments.

[e] Rate coefficients previously reported in ref. 13.

[f] Upper limit assigned to termolecular rate coefficient, association efficiency, and collision complex lifetime; no association was observed.

[g] Rate coefficients previously reported in ref. 11.

TABLE 4. Effect of unsaturation of neutral reactant upon fullerene ion–molecule association reaction efficiency

Reaction[a]	k_c[a]	$k(2)_{obs}$[a]	$k(3)_{obs}$[a]	$k(2)/k_c$[a]	$\tau(\beta = 0.03)$[a]	$\tau(\beta = 1.0)$[a]
$C_{60}^{2+} + CH_3CH_2CN$	4.41	2.5[b]	>22[c]	0.57	>1.5	>0.04
$C_{60}^{2+} + CH_2CHCN$	4.51	0.070[b]	0.61	0.016	0.042	0.0013
$C_{60}^{2+} + CH_3COC_2H_5$	3.06	1.2[d]	10	0.39	1.1	0.032
$C_{60}^{2+} + CH_3COCCH$	2.89	0.13[d]	1.1	0.045	0.12	0.0037
$C_{60}^{2+} + C_3H_8$	1.90	<0.001[e]	<0.008[f]	<0.0006	<0.001	<0.00004
$C_{60}^{2+} + C_3H_6$	1.98	1.3[e]	>10[c]	0.66	>1.5	>0.04
$C_{60}^{2+} + CH_3CCH$	2.27	0.5[e]	3.8	0.22	0.53	0.016
$C_{60}^{2+} + CH_2CCH_2$	1.85	0.08[e]	0.61	0.043	0.10	0.0031

[a] See footnotes *a–f* for Table 1.

[b] Rate coefficients previously reported in ref. 13.

[c] Lower limit assigned to termolecular rate coefficient, association efficiency, and collision complex lifetime; association is presumed to be saturated at the operating pressure of these experiments.

[d] Rate coefficients previously reported in ref. 15.

[e] Rate coefficients previously reported in ref. 11.

[f] Upper limit assigned to termolecular rate coefficient, association efficiency, and collision complex lifetime; association was observed to occur.

Size of the neutral reactant

Association efficiency increases, sometimes dramatically, with increasing molecular size for molecules featuring the same functional groups, as shown in Table 3.

Degree of unsaturation of the neutral reactant

Two different trends are evident in the values reported in Table 4. For hydrocarbons, association efficiency is apparently highest when the hydrocarbon contains one C=C double bond; for functionalized organic molecules such as nitriles and ketones, however, efficiency is highest when the alkyl chain of the molecule is saturated.

Structure of the neutral reactant

Results reported in Table 5 indicate that the efficiency of association of C_{60}^{n+} with different isomers can differ by more than one order of magnitude.

B. Single-well model

We begin with a consideration of the simplest potential energy surface that may be used to describe the association of C_{60}^{n+} with a molecule X: the single-well model shown in Fig. 1. The kinetic and energetic parameters associated with such a model are straightforward and may be used to provide a first-order appreciation of the factors that affect association efficiency. At pressures at which the observed association reaction has not become saturated (i.e., above which collisional stabilization can still increase the efficiency of association), the association efficiency, $k(2)_{obs}/k_c$, is directly related to the lifetime of the collision complex, τ_d, since $k(2)_{obs} = k(3)_{obs}[He]$ and $k(3)_{obs} = k_c k_s \tau_d$. Here $k(3)_{obs}$ is the experimental termolecular rate coefficient for adduct formation, k_c is the theoretical rate coefficient for collision complex formation, and k_s is the theoretical rate coefficient for collisional stabilization.

TABLE 5. Effect of neutral reactant structure upon fullerene ion–molecule association reaction efficiency

Reaction[a]	k_c[a]	$k(2)_{obs}$[a]	$k(3)_{obs}$[a]	$k(2)/k_c$[a]	$\tau(\beta = 0.03)$[a]	$\tau(\beta = 1.0)$[a]
$C_{60}^{\cdot+} + C_2H_5NH_2$	1.34	0.050[b]	0.43	0.037	0.21	0.0064
$C_{60}^{\cdot+} + (CH_3)_2NH$	1.22	0.85[b]	>7.4[c]	0.70	>4	>0.12
$C_{60}^{2+} + C_2H_5OH$	2.77	0.033[d,e]	0.26	0.012	0.030	0.00091
$C_{60}^{2+} + (CH_3)_2O$	2.46	0.003[d]	0.024	0.0012	0.0031	0.000093
$C_{60}^{2+} + CH_3COOH$	2.42	0.40[f]	3.2	0.17	0.42	0.013
$C_{60}^{2+} + HCOOCH_3$	2.43	0.011[f]	0.089	0.0045	0.012	0.00035
$C_{60}^{2+} + CH_3CCH$	2.27	0.50[g]	3.8	0.22	0.53	0.016
$C_{60}^{2+} + CH_2CCH_2$	1.85	0.080[g]	0.61	0.043	0.10	0.0031

[a] See footnotes *a*–*f* for Table 1.

[b] Rate coefficients previously reported in ref. 10.

[c] Lower limit assigned to termolecular rate coefficient, association efficiency, and collision complex lifetime; association is presumed to be saturated at the operating pressure of these experiments.

[d] Rate coefficients previously reported in ref. 14.

[e] Rate coefficient ascribed to adduct formation; a minor channel (10%) leading to hydroxide abstraction was noted also.

[f] Rate coefficients previously reported in ref. 15.

[g] Rate coefficients previously reported in ref. 11.

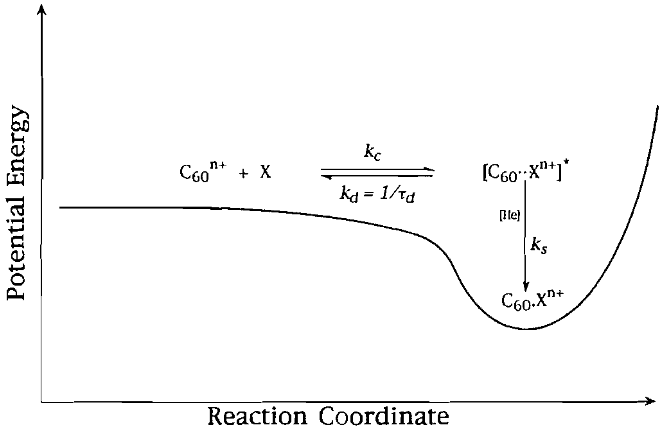

FIG. 1. Schematic diagram of the potential energy surface leading to association, for a single-well model. While such a model may not accurately represent the potential energy surface, consideration of the kinetic parameters involved is straightforward and provides an insight into the factors affecting association efficiency in the reactions of fullerene cations.

The mean lifetime, τ_d, of the collision complex can be determined with the expression

$$[9] \qquad \tau_d = k(3)_{obs}/k_c k_s$$

The usual value assumed for k_c is the ADO collision rate coefficient for this reaction, while k_s is assigned a value $k_s = \beta k_{s(c)}$ where β denotes the efficiency of the collisional stabilization process and $k_{s(c)}$ is the Langevin rate coefficient for collision with helium. In Tables 1–5, which list computed lifetimes, we have used values of $\beta = 0.03$ and 1.0 for the probability of stabilization per collision at 294 K, in the expectation that this range of values encompasses the true probability of collision complex stabilization. The upper limit of $\beta = 1$ is almost certainly unrealistic, since it is unlikely that every collision of a helium atom with the fullerene surface serves to stabilize the chemical bond between the adduct moiety X and one C atom of the fullerene lattice. Ion cyclotron resonance (ICR) studies on a number of association reactions (23, 24) have indicated values of $\beta \leq 0.3$ for helium buffer gas. In any event, we anticipate that β will remain essentially invariant for a series of reactions of fullerene ions C_{60}^{n+} with similar compounds X (for example, the series of nitriles $C_nH_{2n+1}CN$) and so any consistent trend in the calculated complex lifetimes in such a series is expected to be meaningful.

The collision complex lifetime τ_d is generally considered to depend strongly upon the number of degrees of freedom available for energy dispersal, and upon the depth of the potential well for collision complex formation. The expression (25):

$$[10] \qquad \tau_d = \tau_0 \left(\frac{D + 3RT}{3RT} \right)^{s-1}$$

indicates the nature of the expected dependence upon the well depth D and upon the number of degrees of freedom s. Although eq. [10] is overly simplistic in the light of current theoretical investigations of association reactions, we consider that this equation has sufficient qualitative validity to be useful in a consideration of collision complex lifetimes.

What do the computed lifetimes in Tables 1–5 tell us about the features of the single-well potential energy surfaces?

1. The very high apparent dependence of the collision complex lifetime upon charge state, showing a large increase in lifetime with increasing charge state in reactions featuring the same neutral and presumably possessing the same number of degrees of freedom, suggests that the depth of the potential well corresponding to collision complex formation increases substantially with increasing charge state.

2. The substantial enhancement in inferred collision-complex lifetimes for association reactions of C_{56}^{n+} and C_{58}^{n+} (over those apparent for C_{60}^{n+}) can be accounted for, as we have discussed previously (18), by a consideration of the degree of pyramidalization of the carbon atom sites upon the fullerene ion surface. Three types of carbon atom sites can be distinguished for fullerenes, on the basis of the geometry of the surrounding ring system. In Buckminsterfullerene, C_{60}, each C atom forms the apex of one pentagonal and two hexagonal faces (a [C_5, C_6, C_6] site). Other fullerenes also feature such sites, but small fullerenes (C_n, $n < 60$) also contain some

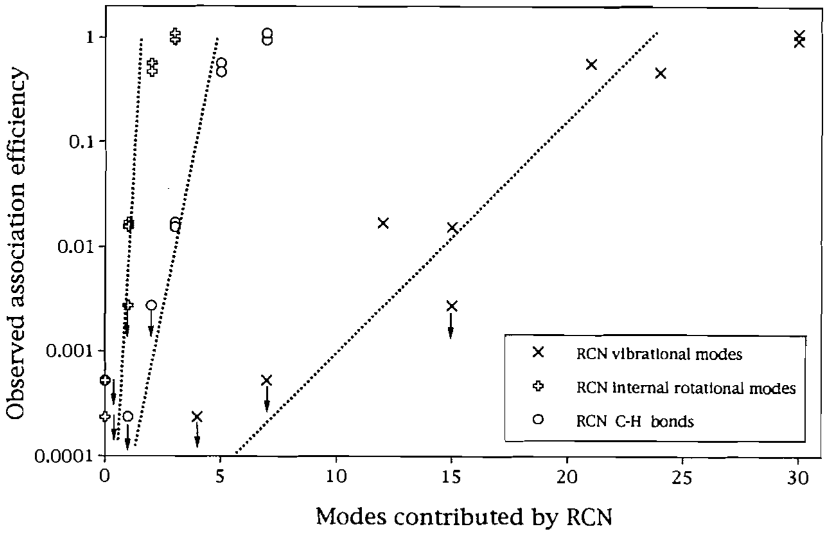

FIG. 2. Graph showing the observed efficiency of the association reaction C_{60}^{2+} + RCN for a variety of nitriles, plotted as a function of the total number of vibrational modes, the number of internal rotational modes, or the number of carbon–hydrogen bonds in the reactant nitrile RCN. Upper limits to the association reactions with HCN, with C_2N_2, and with $CH_2(CN)_2$ are denoted by downward-pointing arrows beside the appropriate symbol. Dotted lines are intended as an aid to visualizing the trends in the data rather than as a quantitative best-fit to the data. The general trend for association efficiency to increase with increasing reactant size is apparent. The kinetic data, which were presented previously in ref. 13, were obtained at 294 ± 2 K at a helium buffer gas pressure of 0.35 ± 0.01 Torr.

[C_5, C_5, C_6] sites, and larger fullerenes ($C_n, n > 60$) feature ($n - 60$) sites of type [C_6, C_6, C_6]. The degree of pyramidalization at the carbon atom in question increases with an increasing proportion of pentagonal C_5 rings. The experimental values reported in Table 2 suggest strongly that the more highly pyramidal [C_5, C_5, C_6] sites found in C_{56}^{n+} and C_{58}^{n+} are substantially more reactive than the [C_5, C_6, C_6] sites of C_{60}^{n+}; there is some indication, also, that the [C_6, C_6, C_6] sites (which have the lowest degree of pyramidalization) are the least reactive, since C_{70}^{n+} is seen to form adducts with a lower efficiency than is C_{60}^{n+}. The depth of the potential well involved in collision complex formation thus appears to be greatest for [C_5, C_5, C_6] sites and smallest for [C_6, C_6, C_6] sites, in keeping with expectations of the amount of distortion necessary at each site to attain tetrahedral coordination of the carbon atom concerned.

3. The trend evident in Table 2 also suggests that the fullerene ion contributes few degrees of freedom to the collison complex. C_{70}^{n+} has 105 C—C bonds whereas C_{60}^{n+} has 90 such bonds; C_{60}^{n+}, despite having fewer vibrational degrees of freedom than C_{70}^{n+}, is seen to associate more efficiently and therefore presumably has a longer-lived collision complex. This observation indicates that the increase in the number of degrees of freedom for C_{70}^{n+} over C_{60}^{n+} is not sufficient to overcome the effect of an apparently shallower potential well.

4. Table 3 indicates that the increasing alkyl substitution of the reactant noticeably increases the collision complex lifetime, presumably by increasing the number of degrees of freedom of the collision complex. Another effect of increasing alkyl substitution is perhaps that of charge stabilization by inductive donation of electrons to the charge site in question (that is, increasing the depth of the potential well). This inductive effect may play a role in the efficiencies seen for $C_{60}^{\cdot+}$ with the series of amines $(CH_3)_nNH_{3-n}$ (n = 0–3) and in the very large change in association efficiency of C_{60}^{2+} with ethylene and with propylene, but inductive charge stabilization cannot account for the trend seen in the nitriles (for example, an increase in the collision complex lifetime by a factor of at least 30 is apparent in the progression from CH_3CN to C_2H_5CN).

The data for the nitriles is also shown in Fig. 2, which plots the observed association efficiency against several molecular parameters for the reactions of C_{60}^{2+} with RCN given in Table 3, as well as for the reactions with the dinitriles C_2N_2 and $CH_2(CN)_2$ and with the unsaturated nitriles CH_2CHCN and CH_2CHCH_2CN. It is apparent from Fig. 2 that, although the general trend is for association efficiency to increase with the total number of substituent vibrational modes, the relation is not monotonic. A better fit is obtained in this instance for the dependence of association efficiency upon the number of C—H bonds within the nitrile, although too few of the reactants RCN exhibit association reactions within the range of efficiences $k(2)/k_c \sim 0.001$–0.3 (that is, above the limit for detection of a reaction by the SIFT technique, and below the expected onset of saturation of the association channel) for the fit to be compelling. These reactions, for which association is the sole observable product channel in all instances studied to date, should occur at lower efficiency at a substantially reduced buffer gas pressure. Therefore, the association reactions of C_{60}^{2+} with the larger nitriles (which occur with high efficiency under SIFT conditions) would seem to be a promising system for further study of association efficiency, using a lower pressure technique such as ICR, which has already been shown capable of detecting fullerene-ion addition products (7, 21, and footnote 2).

5. Association reactions do not occur with saturated hydrocarbons, but are observed with unsaturated hydrocarbons and with functionalized organic molecules (Table 4). This suggests that association involves bond formation without concomitant bond breaking, as we previously discussed elsewhere (11, 12). Also, where a functional group (C═C, or an atom such as O or N featuring a lone pair) is present within the molecule, further unsaturation serves to reduce the apparent collision complex

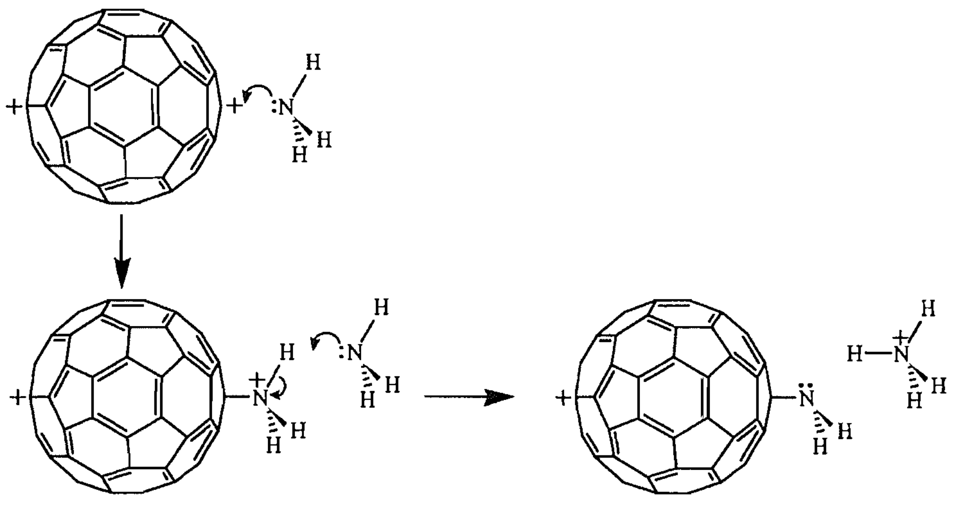

SCHEME 1

lifetime, most probably as a consequence of reduction in the number of available vibrational or internal rotational modes for excess energy dispersal.

6. Substantially different lifetimes are apparent for isomers of organic compounds (Table 5). A number of differing factors may affect the lifetime in such cases: inductive stabilization of charge by a differing number of alkyl groups, steric effects favouring bond formation with one isomer over another, and a difference in the number of effective degrees of freedom (for example, for rotation of alkyl groups in hindered and unhindered complexes). These effects may often occur in competition with each other and are, therefore, best considered on a case-by-case basis since they are not easily accommodated by a simple and general potential energy model for collision complex formation and stabilization.

C. Double-well model

The dependence of association efficiency upon ion charge state, evident in the data shown in Table 1, suggests that the electrostatic interaction between the reactant ion and the neutral is a major component of the collision complex potential well. However, the subsequent reactivity of fullerene adduct ions in several instances, often by proton transfer, (10, 13, 26):

$$[11] \qquad C_{60}\cdot NH_3{}^{2+} + NH_3 \longrightarrow C_{60}\cdot NH_2{}^{+} + NH_4{}^{+}$$

$$[12] \qquad C_{60}\cdot HCN^{\bullet 3+} + HCN \longrightarrow C_{60}\cdot CN^{\bullet 2+} + HCNH^{+}$$

but exhibiting also methyl cation transfer in some cases:

$$[13] \qquad C_{60}\cdot HCOOCH_3{}^{\bullet 3+} + HCOOCH_3 \longrightarrow C_{60}\cdot COOH^{\bullet 2+} + HC(OCH_3)_2{}^{+}$$

is more consistent with the expected reactivity of chemically bonded adducts formed as shown in Scheme 1 than with the likely reactivity of electrostatically bound complexes. The greater facility for complex formation observed with the adjacent-pentagon fullerene ions $C_{56}{}^{n+}$ and $C_{58}{}^{n+}$ than with the isolated-pentagon ions $C_{60}{}^{n+}$ and $C_{70}{}^{n+}$ is suggestive of tetrahedral coordination at the site of addition and therefore also supports covalent bond formation. It thus appears likely that the potential energy surface may involve two minima rather than a single potential well. A double-well surface of this type is shown in Fig. 3. Nevertheless, we stress that the evidence favouring a double-well potential surface over a single-well model is rather circumstantial.

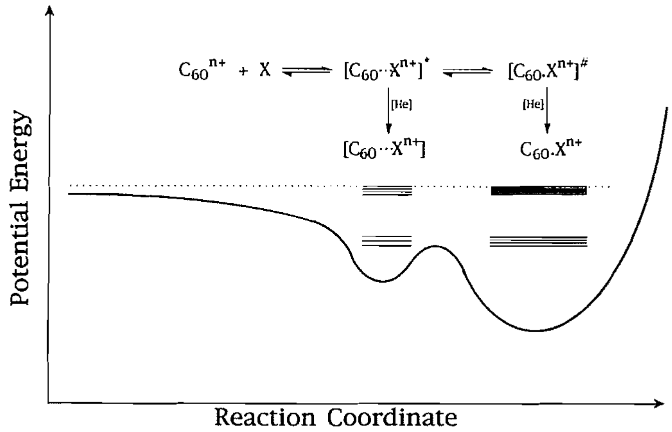

FIG. 3. Schematic diagram of the potential energy surface leading to association, for a double-well model. The barrier between the electrostatically bound complex, $[C_{60}\cdots X^{n+}]$, which is expected to correspond to the initial structure of the collision complex, and the covalently bonded adduct, $[C_{60}\cdot X^{n+}]$, is considered to arise from the energetic requirement to distort the fullerene surface in order to achieve sp^3 hybridization at the carbon atom involved in bond formation. The dotted line shows the total thermal and potential energy of reactants; also shown schematically are the relative densities of states for the electrostatically bound complex and the covalently bonded adduct at the total energy of reactants and at the height of the submerged barrier. The density of states ratio is expected to consistently favour covalent bond formation, since this potential well is expected to have greater depth.

A possible rationalization for the existence of a barrier between the electrostatically bound collision complex and the covalently bonded adduct is the necessity to distort the fullerene carbon framework at the site of the fullerene-substituent bond formation, so as to achieve sp^3 hybridization at this site on the fullerene surface. Such a barrier would presumably be more easily traversed for the adjacent-pentagon [C_5, C_5, C_6] charge sites in $C_{56}{}^{n+}$ and $C_{58}{}^{n+}$ (which, on geometric grounds, are expected to have a comparatively high degree of pyramidalization, and of sp^3 character, prior to interaction with the re-

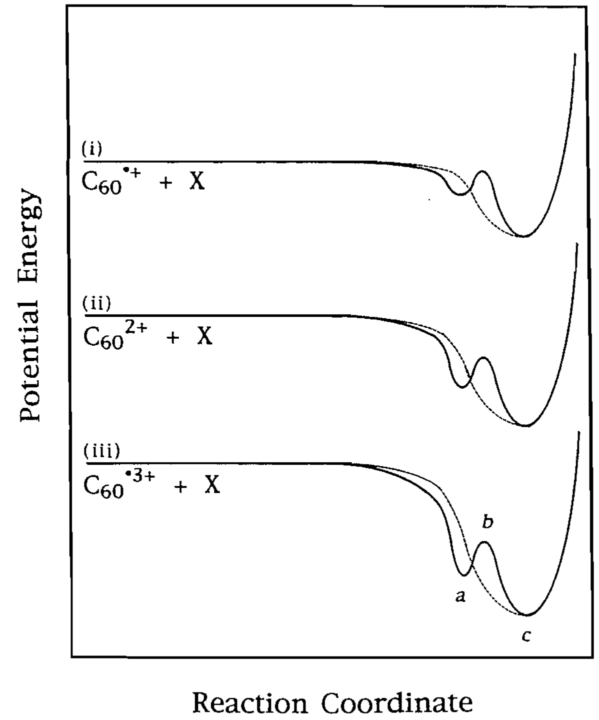

FIG. 4. Schematic diagram illustrating the increasing depth of the potential well(s) leading to adduct formation, and of the barrier to covalent bond formation in the double-well model, with increasing charge state.

actant neutral) than for the charge sites in C_{60}^{n+} and larger fullerenes: this can account for the observed trend (Table 2) for fullerene ion sizes. Traversal of the barrier should also be more facile for collision complexes having a higher charge state, since the barrier height (relative to the electrostatic well depth) should be essentially independent of charge state while the electrostatic well depth will increase with charge state. We have illustrated this point schematically in Fig. 4.

The double-well model provides for the collisional stabilization of the electrostatically bound collision complex as well as of the chemically bonded adduct, and thus two isomeric structures of the association product are possible. We have not yet observed any evidence (upon the basis of subsequent reactivity) that supports this possibility: however, if the well depth for chemical bond formation is substantially greater than the depth of the electrostatic well as we have suggested, then the density of states in the energy window above the barrier to interconversion is expected to consistently favour chemical bond formation and so the chemically bonded adduct should be the major product of the association reaction provided that the collision complex is sufficiently long-lived to allow an equilibrium to be attained between the two minima.

Several other examples can be found in the literature, of reaction processes in positive ion – molecule chemistry involving discrete potential wells for electrostatically and covalently bound complexes. The negative temperature dependence observed for the methyl cation transfer reaction

[14] $(CH_3)_2Cl^+ + C_6H_5CH_3 \longrightarrow C_6H_5(CH_3)_2^+ + CH_3Cl$

suggests that this exothermic reaction occurs on a surface involving at least two minima (27), and studies of other alkyl cation transfer reactions of dialkylchloronium ions (28–31) also indicate that a barrier exists between electrostatic complex formation and the transition to a covalently bonded adduct.

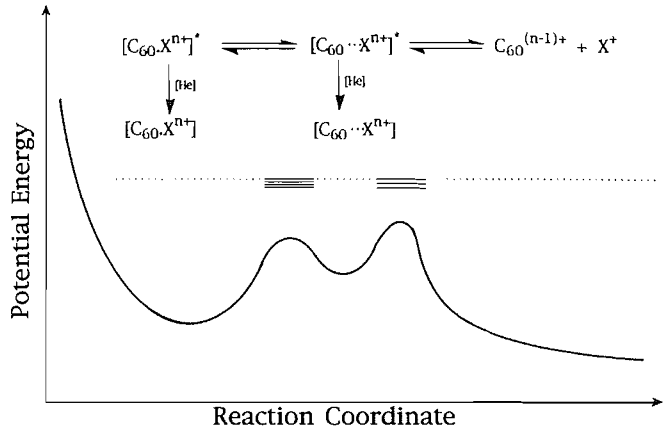

FIG. 5. Schematic diagram illustrating the potential energy surface involved in the competition between covalently bonded adduct formation and accessible charge transfer in the reaction of a polycation C_{60}^{n+} and a neutral X. For simplicity, the channel leading back from the (electrostatically bound) collision complex $[C_{60}\cdots X^{n+}]^*$ to reactants has not been included. Covalent bond formation can only compete effectively with charge transfer if the density of states above the (submerged) barrier to bond formation exceeds that above the (submerged) Coulombic barrier to charge transfer from a polycation: the occurrence of such competition in a reaction thus provides a lower limit to the depth of the potential well in the reaction concerned.

Similar potential energy surfaces have been proposed to explain the observed reactivity of gas-phase electrophilic aromatic substitution reactions (32, 33). The kinetics of ferrocene protonation (34):

[15] $BH^+ + Fe(C_5H_5)_2 \longrightarrow Fe(C_5H_5)_2H^+ + B$

are similarly indicative of a barrier between electrostatically bound and covalently bonded adduct structures: this barrier is interpreted as arising from a change in geometry upon protonation. These examples demonstrate that the existence of barriers to bond formation in ion–molecule reactions may be rather common, especially when bond formation necessitates substantial distortion or deformation of the reactants.

D. Competition with charge transfer

The occurrence of association becomes a more complex issue in the presence of a competing exothermic bimolecular product channel such as charge transfer. This is especially true for reactions of the multiply charged ions C_{60}^{2+} and $C_{60}^{\cdot 3+}$, since charge separation reactions of such ions are inhibited by a substantial reverse activation energy barrier δ arising from the Coulombic repulsion between the product ions, which are initially formed in close mutual proximity (20, 35, 36). We have presented elsewhere a model for the potential energy surface involved in charge separation reactions of fullerene ions (37), which indicates a barrier height of $\delta = 1.80 \pm 0.16$ eV for reactions of the type

[16] $C_{60}^{2+} + X \longrightarrow C_{60}^{\cdot+} + X^{\cdot+}$

and $\delta = 4.5 \pm 0.4$ eV for the reactions

[17] $C_{60}^{\cdot 3+} + X \longrightarrow C_{60}^{2+} + X^{\cdot+}$

We have observed association reactions in competition with accessible charge transfer. Several reactions of this type are listed in Table 6. If our proposal of a double-well model is correct, then such reactions provide some indication of the relative barrier heights (in the forward direction) for chemical

TABLE 6. Reactions exhibiting competition between association and charge transfer

Reaction	IE(X)[a]	$-(\Delta H^0 + \delta)$[b]	$\mathrm{B.R.}_{\mathrm{assn}}$[c]	$\mathrm{B.R.}_{\mathrm{ct}}$[c]	$k(2)_{\mathrm{obs}}$[d]	k_{c}[e]
C_{60}^{2} + $(C_2H_5)_2O$[f]	9.51 ± 0.01	0.08	0.1	0.9	0.91	2.30
C_{60}^{2+} + c-C_4H_8O[f]	9.41 ± 0.02	0.18	0.6	0.4	1.9	2.50
C_{60}^{2+} + $CH_3COC_3H_7$[g]	9.38 ± 0.01	0.21	0.9	0.1	1.8	2.99
C_{60}^{2+} + $(C_2H_5)_2CO$[g]	9.31 ± 0.01	0.28	0.75	0.25	1.9	2.99
C_{60}^{2+} + c-C_5H_8O[g]	9.25 ± 0.01	0.34	0.3	0.7	2.8	3.31
C_{60}^{2+} + $(CH_3)_2CCH_2$[h]	9.239 ± 0.003	0.35	0.9	0.1	2.4	2.03
C_{60}^{2+} + (Z)-2-C_4H_8[h]	9.108 ± 0.008	0.48	0.2	0.8	3.4	1.96
C_{60}^{2+} + C_4H_6[h]	9.07[i]	0.52	0.8	0.2	1.0	1.94
C_{60}^{2+} + CH_3NH_2[j]	8.97 ± 0.02	0.62	0.9	0.1	2.6	2.68
C_{60}^{2+} + $C_2H_5NH_2$[j]	8.86 ± 0.02	0.73	0.7	0.3	2.6	2.68
C_{60}^{2+} + $(CH_3)_2NH$[j]	8.23 ± 0.08	1.36	0.1	0.9	2.9	2.44
$C_{60}^{\cdot 3+}$ + CH_2CHCN[k]	10.91 ± 0.01	0.18	0.9	0.1	4.0	6.77
$C_{60}^{\cdot 3+}$ + CH_3OH[f]	10.85 ± 0.01	0.24	0.2	0.8	2.5	4.38
$C_{60}^{\cdot 3+}$ + $HCOOCH_3$[g]	10.815 ± 0.005	0.28	1.0	0	2.9	3.65
$C_{60}^{\cdot 3+}$ + CH_3COOH[g]	10.66 ± 0.02	0.43	1.0	0	4.2	3.63
$C_{60}^{\cdot 3+}$ + CH_3COOCH_3[g]	10.27 ± 0.02	0.82	0.9	0.1	3.4	3.50
$C_{60}^{\cdot 3+}$ + CH_2CHCH_2CN[k]	10.20 ± 0.05	0.89	0.6	0.4	6.6	5.81
$C_{60}^{\cdot 3+}$ + CH_3COCCH[g]	10.17 ± 0.02	0.92	0.2	0.8	4.5	4.33
$C_{60}^{\cdot 3+}$ + NH_3[j]	10.16 ± 0.01	0.93	1.0	0	1.2	3.37
$C_{60}^{\cdot 3+}$ + C_2H_5CHO[g]	9.953 ± 0.05	1.14	0.25	0.75	4.2	4.72

[a] Ionization energy (in eV) of the reactant neutral, obtained from the tabulation of Lias et al. (38) unless otherwise indicated.

[b] Calculated depth of the submerged barrier to charge transfer, obtained as the difference between the observed threshold to charge transfer (IE = 9.59 ± 0.11 eV for C_{60}^{2+}, IE = 11.09 ± 0.09 eV for $C_{60}^{\cdot 3+}$) 20, 36, 37, and IE(X).

[c] Experimentally obtained branching ratios (±30%) for association and for charge transfer, respectively.

[d] Observed effective bimolecular rate coefficient for addition, in units of 10^{-9} cm^3 $molecule^{-1}$ s^{-1}.

[e] ADO collision rate coefficient in units of 10^{-9} cm^3 $molecule^{-1}$ s^{-1}, calculated according to the method of Su and Bowers (19).

[f] Results previously reported in ref. 14.

[g] Results previously reported in ref. 15.

[h] Results previously reported in ref. 11.

[i] Reported in ref. 39.

[j] Results previously reported in ref. 10.

[k] Results previously reported in ref. 13.

bond formation and for charge transfer as we have illustrated in Fig. 5. The experimental results obtained to date show that association is able to compete to some extent with charge transfer reactions whose exothermicity exceeds the threshold value δ by up to ~0.6 eV for reactions of C_{60}^{2+}, and up to ~1.0 eV for $C_{60}^{\cdot 3+}$. At first glance there appears little evidence of a clear trend between exothermicity of charge transfer and the observed branching ratio for charge transfer, but this is understandable given the wide range in addition efficiencies that could be expected for these compounds in the absence of a competing charge transfer channel. For example, our studies of amine, nitrile, alcohol, and ketone addition reactions with C_{60}^{n+} indicate that nitrogen-containing nucleophiles (especially amines) are substantially more efficient at forming adducts than are the oxygen-containing nucleophiles (especially ethers). If these intrinsic differences in addition efficiency are taken into consideration, it is possible to discern a tendency (in any given class of compounds) for charge transfer to become dominant as it becomes sufficiently exothermic, as would be expected.

The results listed in Table 6 suggest that the barrier to bond formation for these reactions is submerged by at least 0.6 eV and 1.0 eV for doubly and triply charged ions, respectively. This places, also, a lower limit on the collision complex well depth in these examples (since this depth must exceed that of the submerged barrier to bond formation, if the double-well model is correct). If the collision complex well depth arises solely from the electrostatic and ion–dipole attractions between a (point-charge) fullerene ion and the neutral reactant in question, these lower limits indicate a separation of the reactants in the collision complex of no greater than 4.8 Å for C_{60}^{2+}+CH_3NH_2 and 4.5 Å for $C_{60}^{\cdot 3+}$ + NH_3. This distance restriction does not appear unreasonably restrictive — such a separation does not necessitate bond formation between the reactants. However, it is not clear how well the fullerene polycations conform to such a point-charge model: certainly the magnitude of the reverse activation energy barrier to charge transfer is better accommodated (in the case of charge transfer from C_{60}^{2+} and, we anticipate, from $C_{60}^{\cdot 3+}$) by assuming that the charges upon the fullerene polycation are initially as widely separated as is possible on the surface of a 7.0 Å spheroid. If the fullerene ion is not treated as a point charge, the required separation between the ion and the neutral (to produce an electrostatic well of greater depth than the submerged barrier to charge transfer) will be substantially less than the maximum separation permitted by a point-charge model.

Conclusions

The efficiency of association reactions of fullerene cations observed to occur in helium at the comparatively high pressures (0.35–0.4 Torr) sustained in a SIFT apparatus at room temperature has been scrutinized in terms of the influence of the charge state and the size of the fullerene ion and the size, structure, and degree of unsaturation of the neutral. The association efficiency is found to be strongly dependent on these molecular parameters. The magnitude of the efficiency, when translated into the lifetime of an intermediate collision complex, provides insight into the well depth associated with the formation of this complex and the effectiveness of vibrational and (or) rotational degrees of freedom in the fullerene cation and the added neutral molecule in the dispersal of the excess energy of the complex.

The observed results are considered in the light of a single-well and a double-well model for the potential energy surface leading to association, but they are best accommodated by the double-well model involving the formation of an initial electrostatic collision complex, which must overcome a barrier (corresponding to the energetic requirement for localized surface deformation) to proceed to the formation of a chemically bonded adduct. The observation of competition of association with charge transfer can also be accommodated with a double-well model, which provides a lower limit for the depth of the electrostatic well for those systems that exhibit such competition. More insight into the nature of the potential energy surface would be provided by more detailed investigations of the pressure dependence (including the very low pressure regime) and of the influence of temperature upon association efficiency. Investigation of the chemistry of higher charge states such as $C_{60}{}^{4+}$ and $C_{56}{}^{\bullet 5+}$ may also yield further information on the factors governing association reactions of fullerene ions.

The discussion of the models for the potential energy surfaces associated with fullerene-adduct formation is necessarily rather qualitative in nature. Several theoretical models do exist that treat, in a quantitative or semi-uantitative fashion, features of the potential energy surfaces for radiatively and collisionally stabilized association reactions (40). However, these models generally require a reasonably detailed knowledge of the exothermicity of adduct formation and the vibrational frequencies of the collision complex. In the present context, the thermochemistry of derivatized ionized fullerenes is as yet virtually unknown, and the ab initio calculation of vibrational spacings for a derivatized fullerene ion $C_{60}{\cdot}X^{n+}$ requires a major investment in computing time: at present, no such calculations have been reported. It is, therefore, not yet possible to model theoretically the efficiency of fullerene ion addition reactions, although such an aim is certainly desirable to augment or critically assess the models for the potential energy surface for association that we have presented here.

Acknowledgements

D.K.B. thanks the Natural Sciences and Engineering Research Council of Canada for the financial support of this research and the Canada Council for a Killam Research Fellowship.

1. J.M. Farrar and W.H. Saunders, Jr. (*Editors*). Techniques for the study of ion–molecule reactions. Techniques of Chemistry. Vol. XX. Wiley–Interscience, New York. 1988.
2. D.K. Bohme. *In* Structure/reactivity and thermochemistry of ions. *Edited by* P. Ausloos and S.G. Lias. Reidel, Dordrecht, The Netherlands. 1987. p. 219.
3. K.G. Spears and F.C. Fehsenfeld. J. Chem. Phys. **56**, 5698 (1972).
4. L.M. Roth and B.S. Freiser. Mass Spectrom. Rev. **10**, 303 (1991).
5. R. Tonkyn and J.C. Weisshaar. J. Am. Chem. Soc. **108**, 7128 (1986).
6. W. Krätschmer, L.D. Lamb, K. Fostiropoulos, and D.R. Huffman. Nature, **347**, 354 (1990).
7. S.W. McElvany and S.B.H. Bach. 39th Conf. Mass Spectrom. Allied Topics, Nashville, Tenn. 1991. p. 422.
8. S.W. McElvany, M.M. Ross, and J.H. Callahan. Acc. Chem. Res. **25**, 162 (1992).
9. H. Schwarz, T. Weiske, D.K. Bohme, and J. Hrusak. *In* Buckminsterfullerenes. *Edited by* W.E. Billups and M.A. Ciufolini. VCH, New York. 1993. p. 257.
10. (*a*) G. Javahery, S. Petrie, A. Ketvirtis, J. Wang, and D.K. Bohme. Int. J. Mass Spectrom. Ion Processes, **116**, R7 (1992); (*b*) G. Javahery, S. Petrie, H. Wincel, J. Wang, and D.K. Bohme. J. Am. Chem. Soc. **115**, 5716 (1993).
11. S. Petrie, G. Javahery, J. Wang, and D.K. Bohme. J. Am. Chem. Soc. **114**, 9177 (1992).
12. S. Petrie, G. Javahery, and D.K. Bohme. J. Am. Chem. Soc. **115**, 1445 (1993).
13. G. Javahery, S. Petrie, J. Wang, H. Wincel, and D.K. Bohme. J. Am. Chem. Soc. **115**, 9701 (1993).
14. G. Javahery, S. Petrie, H. Wincel, J. Wang and D.K. Bohme. J. Am. Chem. Soc. **115**, 6295 (1993).
15. S. Petrie, G. Javahery, H. Wincel, J. Wang and D.K. Bohme. Int. J. Mass Spectrom. Ion Processes. In press.
16. J. Wang, G. Javahery, S. Petrie, and D.K. Bohme. J. Am. Chem. Soc. **114**, 9665 (1992).
17. H. Becker, G. Javahery, S. Petrie, P.-C. Cheng, H. Schwarz, L.T. Scott, and D.K. Bohme. J. Am. Chem. Soc. **115**, 11636 (1993).
18. S. Petrie and D.K. Bohme. Nature, **365**, 426 (1993).
19. T. Su and M.T. Bowers. Int. J. Mass Spectrom. Ion Phys. **12**, 347 (1973).
20. G. Javahery, H. Wincel, S. Petrie, and D.K. Bohme. Chem. Phys. Lett. **204**, 467 (1993).
21. S.W. McElvany, M.M. Ross, and J.H. Callahan. Mater. Res. Soc. Symp. Proc. **206**, 697 (1991).
22. J.J. Stry, M.T. Coolbaugh, E. Turos, and J.F. Garvey. J. Am. Chem. Soc. **114**, 7914 (1992).
23. P.R. Kemper, L.M. Bass, and M.T. Bowers. J. Phys. Chem. **89**, 1105 (1985).
24. M.J. McEwan, A.B. Denison, V.G. Anicich, and W.T. Huntress. Int. J. Mass Spectrom. Ion Processes, **81**, 247 (1987).
25. A. Good. Trans. Faraday Soc. **67**, 3495 (1971).
26. S. Petrie, G. Javahery, and D.K. Bohme. Int. J. Mass Spectrom. Ion Processes, **124**, 145 (1993).
27. D.K. Sen Sharma and P. Kebarle. J. Am. Chem. Soc. **104**, 19 (1982).
28. T.F. Magnera and P. Kebarle. *In* Ionic processes in the gas phase. *Edited by* M.A. Almoster Ferreira. Reidel, Dordrecht, The Netherlands. 1982. p. 135.
29. P.J. Mathews and J.A. Stone. Can. J. Chem. **66**, 1239 (1988).
30. M. Speranza and G. Laguzzi. J. Am. Chem. Soc. **110**, 30 (1988).
31. M. Attina, F. Cacace, and A. Ricci. Angew. Chem. Int. Ed. Engl. **30**, 1457 (1991).
32. F. Cacace, M.E. Crestoni, A. Dimarzio, and S. Fornarini. J. Phys. Chem. **95**, 8731 (1991).
33. M. Attina and F. Cacace. Gazz. Chim. Ital. **118**, 241 (1988).
34. M.G. Ikonomou, P. Kebarle, and J. Sunner. J. Phys. Chem. **92**, 6308 (1988).
35. L.M. Roth and B.S. Freiser. Mass Spectrom. Rev. **10**, 303 (1991).
36. S. Petrie, G. Javahery, J. Wang, and D.K. Bohme. J. Phys. Chem. **96**, 6121 (1992).
37. S. Petrie, J. Wang, and D.K. Bohme. Chem. Phys. Lett. **204**, 473 (1993).
38. S.G. Lias, J.E. Bartmess, J.F. Liebman, J.L. Holmes, R.D. Levin, and W.G. Mallard. J. Phys. Chem. Ref. Data, **17**, Suppl. no. 1 (1988).
39. R.C. Weast (Editor). CRC handbook of chemistry and physics CRC Press, Boca Raton, Fla. 1986.
40. (*a*) D.R. Bates and E. Herbst. *In* Rate coefficients in astrochemistry. *Edited by* T.J. Millar and D.A. Williams. Kluwer, Dordrecht, The Netherlands. 1988. p. 17; (*b*) R.C. Dunbar. Int. J. Mass Spectrom. Ion Processes, **100**, 423 (1990); (*c*) E. Herbst and R.C. Dunbar. Mon. Not. R. Aston. Soc. **253**, 341 (1991); (*d*) S.C. Smith, M.J. McEwan, and R.G. Gilbert. J. Chem. Phys. **90**, 1630 (1989).